Exotic mesons in quenched lattice QCD

Claude Bernard and James E. Hetrick
Department of Physics, Washington University, St. Louis, Missouri 63130

Thomas A. DeGrand and Matthew Wingate
Physics Department, University of Colorado, Boulder, Colorado 80309

Carleton DeTar and Craig McNeile
Physics Department, University of Utah, Salt Lake City, Utah 84112
and Zentrum für Interdisziplinäre Forschung, Universität Bielefeld, Bielefeld, Germany

Steven Gottlieb
Department of Physics, Indiana University, Bloomington, Indiana 47405

Urs M. Heller
SCRI, Florida State University, Tallahassee, Florida 32306-4130

Kari Rummukainen
Universität Bielefeld, Fakultät für Physik, Postfach 100131, D-33501 Bielefeld, Germany

Bob Sugar
Department of Physics, University of California, Santa Barbara, California 93106

Doug Toussaint
Department of Physics, University of Arizona, Tucson, Arizona 85721
and Center for Computational Physics, University of Tsukuba, Ibaraki 305, Japan

Since gluons in QCD are interacting fundamental constituents just as quarks are, we expect that in addition to mesons made from a quark and an antiquark, there should also be glueballs and hybrids (bound states of quarks, antiquarks, and gluons). In general, these states would mix strongly with the conventional $\bar{q}q$ mesons. However, they can also have exotic quantum numbers inaccessible to $\bar{q}q$ mesons. Confirmation of such states would give information on the role of ''dynamical'' color in low energy QCD. In the quenched approximation we present a lattice calculation of the masses of mesons with exotic quantum numbers. These hybrid mesons can mix with four quark ($\bar{q}\bar{q}qq$) states. The quenched approximation partially suppresses this mixing. Nonetheless, our hybrid interpolating fields also couple to four quark states. Using a four-quark source operator, we demonstrate this mixing for the 1^{-+} meson. Using the conventional Wilson quark action, we calculate both at reasonably light quark masses, intending to extrapolate to small quark mass, and near the charmed quark mass, where we calculate the masses of some $\bar{c}cg$ hybrid mesons. The hybrid meson masses are large — over 4 GeV for charmonium and more than twice the vector meson mass at our smallest quark mass, which is near the strange quark mass. [S0556-2821(97)06123-7]

PACS number(s): 12.38.Gc, 12.39.Mk

I. INTRODUCTION

While there is a long history of glueball mass calculations in lattice QCD, including attempts to use lattice calculations to identify experimentally observed mesons with glueballs [1,2], hybrid mesons have received much less attention. These bound states of quarks and gluons have been treated in a variety of approximations to QCD, including the bag model, flux-tube model, and QCD sum rules [3]. As with glueball candidates, a hybrid characterization of an observed state is more convincing if there is not only a match in mass, but also in decay branching ratios. Since the occurrence of hybrid states is obviously a nonperturbative phenomenon, and since lattice gauge theory provides an *ab initio* nonper-turbative formulation of QCD, in principle lattice gauge theory is the ideal method for calculating their properties. One hopes that lattice methods will eventually provide reliable masses and branching ratios, as well as providing a basis for testing the various approximations to QCD.

Although in principle the lattice approach is ideal, in practice there are some difficulties. On the lattices used here, the hybrid masses are large compared to the lattice spacing, and so lattice spacing errors are a serious problem. Also, the propagators are noisy, although perhaps not so much as glueball propagators. This means that we do not have long plateaus in the effective mass, and we must extract mass estimates from rather short distances. While we will end by making the best mass estimates we can, at this stage we are
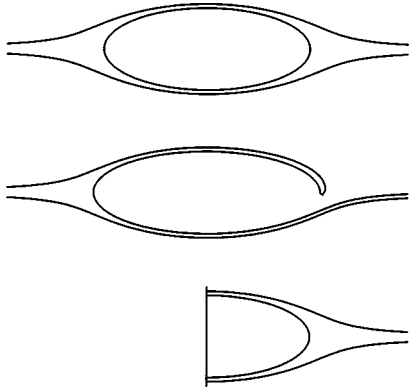
FIG. 1. Quark line diagrams showing mixing with sea quarks (top), ''hairpin'' diagrams mixing hybrid and $\bar{q}\bar{q}qq$ states in the quenched approximation (center), and an off-diagonal propagator with a four-quark source and a hybrid sink (bottom). The vertical line indicates two meson operators at the same Euclidean time but different spatial coordinates.

still exploring methods and the dependence of the results on parameters such as the lattice spacing and quark mass.

The earliest lattice calculations of hybrid mesons used static quarks, where hybrid states appear as excitations of the gluonic string [4]. Also in an early study, the UKQCD Collaboration studied hybrid states in the Υ system, in a simulation of nonrelativistic QCD [5]. More recently, the UKQCD group has presented results in the quenched approximation for quark masses about equal to the strange quark mass [6,7] and we have presented preliminary results using Wilson valence quarks and Kogut-Susskind sea quarks [8].

Hybrid mesons can have the same quantum numbers as conventional $\bar{q}q$ mesons and would be expected to mix strongly with them. (This mixing was demonstrated in Ref. [8].) In addition, hybrid mesons can have exotic quantum numbers. Flavor nonsinglet hybrids with exotic quantum numbers are especially interesting because they cannot mix either with ordinary mesons or with glueballs. They can, however, mix with four-quark ($\bar{q}\bar{q}qq$) states. In the quenched approximation mixing of hybrids and four-quark states through sea quark loops (Fig. 1, top) is not present. However, the hybrid interpolating operators may still couple to four-quark states through ''hairpin'' diagrams (Fig. 1, middle). This coupling can be investigated by using four-quark source operators (Fig. 1, bottom), and we find that it can even be a useful tool in computing the mass of the exotic mesons.

Because of the partial suppression of mixing with four-quark states and because we have a supply of quenched lattices at several lattice spacings, we have calculated exotic meson propagators in the quenched approximation at $6/g^2 = 5.85$ and 6.15. We have done this at a set of quark masses greater than or about equal to the strange quark mass, and at approximately the charmed quark mass.

II. HYBRID OPERATORS AND PROPAGATOR COMPUTATIONS

To make an operator which creates a hybrid meson, we combine a quark, an antiquark, and the color electric or mag-

netic field to form a color singlet with the desired spin, parity, and charge conjugation. We construct these operators by combining representations of the continuum rotation group. An alternative approach using the symmetry group of the hypercubic lattice was presented by Mandula [9] and is also developed in Ref. [6].

Our hybrid operators have the generic structure $\bar{\psi}^a \Gamma \psi^b F^{ab}$, where a and b are triplet color indices, Γ is some combination of Dirac matrices and derivatives, and F is the color electric or magnetic field, a color octet. Because we do not include ''quark-line-disconnected'' diagrams in our propagator, all our meson propagators are flavor non-singlets.

The color electric and magnetic fields have $J^{PC} = 1^{--}$ and 1^{+-}, respectively. The spin, parity, and charge conjugation from the quark and antiquark are those of the available quark bilinears, listed here along with the corresponding mesons. The 0^{+-} bilinear $\bar{\psi}\gamma_0\psi$ does not correspond to a $\bar{q}q$ state. Instead, it is the charge corresponding to a conserved current, the baryon number. Therefore we expect $\int d^3x\, \bar{\psi}\gamma_0\psi|0\rangle = 0$. We may, however, calculate the propagator for this exotic operator or use this bilinear as part of our toolkit for constructing hybrid operators:

$$
\begin{array}{ll}
0^{++}(\bar{\psi}\psi) & (a_0), \\
0^{+-}(\bar{\psi}\gamma_0\psi) & (J_B), \\
0^{-+}(\bar{\psi}\gamma_5\psi, \bar{\psi}\gamma_5\gamma_0\psi) & (\pi), \\
1^{++}(\bar{\psi}\gamma_5\gamma_i\psi) & (a_1), \\
1^{+-}(\bar{\psi}\gamma_5\gamma_0\gamma_i\psi) & (b_1), \\
1^{--}(\bar{\psi}\gamma_i\psi, \bar{\psi}\gamma_i\gamma_0\psi) & (\rho).
\end{array}
$$

We can also give the quark and antiquark a relative orbital angular momentum. This may be useful because in the non-relativistic quark model the a_1 (1^{++}), and hence the 0^{+-} and 0^{--} hybrids constructed below, is a P-wave state. The operator $\overleftrightarrow{\partial}_i = \overrightarrow{\partial}_i - \overleftarrow{\partial}_i$ inserted in the quark bilinear brings in quantum numbers 1^{--}, where the negative charge conjugation comes because C interchanges the quark and antiquark. Thus, a P-wave operator with a_1 quantum numbers 1^{++} is $\epsilon_{ijk}\bar{\psi}\gamma_j\overleftrightarrow{\partial}_k\psi$. This operator may be advantageous because it couples the ''large'' components of the quark spinor to the large components of the antiquark spinor.

For $F_{\mu\nu}$ we use a ''pointlike'' construction, illustrated in Fig. 2. Each open loop represents the product of the links, minus the adjoint of the product. To improve the overlap of the operator with the hybrid meson, we can replace each link by a ''smeared'' link, as illustrated on the right side of the figure. The smeared link is the sum of the single link plus the three link paths displaced in the spatial directions, and so there are four such staples for a link in a spatial direction and six for a link in the time direction. We have experimented with including staples displaced in the time direction in the smearing and found that this distorts the propagators at short distances, and we will be including short distances in our fits. In our earlier work on two-flavor lattices we found that iter-
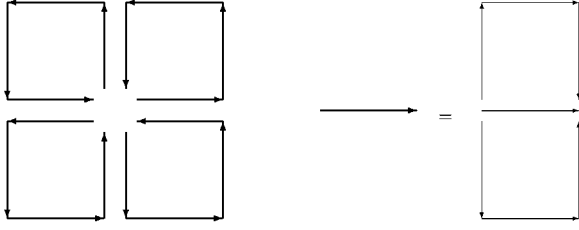
FIG. 2. ''Pointlike'' construction of $F_{\mu\nu}$. Each open loop represents the product of the links, minus the adjoint of the product. Each of these links may actually be a ''smeared'' link, as illustrated on the right side of the figure.

ating the smearing twice gave a slightly better signal than a single smearing, but that four iterations of the smearing was worse. Therefore we have smeared twice in this work. We do expect that as the physical lattice spacing is decreased more iterations of smearing would be advantageous.

Table I shows the various source and sink operators we have used. To construct a meson propagator, we first fixed the gauge to the lattice Coulomb gauge. We then constructed a wall source on one time slice, with a 1 at each lattice point for one color and spin component. A quark propagator was constructed by computing M^{-1} times this source. Then the wall source was multiplied by the source operator, which involved multiplication by Dirac matrices and components of the field strength. The result of this was used as a source for an inversion to compute the antiquark propagator. (This involves an extra γ_5 at each end of the propagator, from the standard identity $M^{\dagger}=\gamma_5 M^* \gamma_5$.) Finally, at each lattice

point the antiquark propagator was multiplied by the desired sink operator and dotted with the quark propagator. The result was summed over each time slice to get the zero momentum mesons.

The first three operators in Table I are standard operators for the 0^{-+}, 1^{--}, and 1^{++} $\bar{q}q$ mesons. We will call these the ''π,'' ''ρ,'' and ''a_1,'' respectively. However, our valence quarks are really much heavier than the physical u and d quarks, and so they might be better thought of as $\bar{s}s$ or, in one case, $\bar{c}c$ mesons. The fourth operator is a P-wave operator for the a_1. In the nonrelativistic quark model the a_1 is a P-wave state, and so the operator with the spatial derivative will connect large components of the Dirac spinor to large components and may give a better signal. This argument also applies to the hybrid operators that we will construct using this quark bilinear as a building block.

The next set of operators are hybrid operators with the same quantum numbers as $\bar{q}q$ operators. In our previous work we verified, by computing propagators with a hybrid operator at one end and a $\bar{q}q$ operator at the other, that these hybrids mix with the corresponding $\bar{q}q$ operators (and do not mix with other quantum numbers) [8]. The ''mnemonic'' column of the table indicates how the operator is constructed. For example, the first hybrid operator, which has pion quantum numbers, can be considered as a quark and antiquark in a 1^{--} or ρ state (but a color octet) combined with a color magnetic field, which has $J^{PC}=1^{+-}$, to make a $J=0$ color singlet object.

TABLE I. Source and sink operators used for our propagators. The first column lists the name used for the operator in the text, and the second column lists the angular momentum, parity, and charge conjugation. The third column is a shorthand indicating how the operator is constructed. In particular, the hybrid operators are constructed from one of the quark bilinear operators from the top block, combined with either the color electric or color magnetic field. The last column lists the actual operator. In this column, a and b are color indices, i, j, and k Cartesian indices, and α, β, and λ are flavor indices included to indicate how the propagators are connected.

Name	J^{PC} (particle)	Mnemonic	Operator
π	0^{-+} (π)	$\bar{q}q$ pion	$\bar{\psi}^a \gamma_5 \psi^a$
ρ	1^{--} (ρ)	$\bar{q}q$ rho	$\bar{\psi}^a \gamma_i \psi^a$
a_1	1^{++} (a_1)	$\bar{q}q$ a_1	$\bar{\psi}^a \gamma_5 \gamma_i \psi^a$
$a_1(P)$	1^{++} (a_1)	P-wave a_1	$\epsilon_{ijk} \bar{\psi}^a \gamma_j \overleftrightarrow{\partial}_k \psi^a$
0_H^{-+}	0^{-+} (π)	$\rho \otimes B$	$\epsilon_{ijk} \bar{\psi}^a \gamma_i \psi^b F_{jk}^{ab}$
1_H^{--}	1^{--} (ρ)	$\pi \otimes B$	$\epsilon_{ijk} \bar{\psi}^a \gamma_5 \psi^b F_{jk}^{ab}$
1_H^{++}	1^{++} (a_1)	$\rho \otimes E$	$\epsilon_{ijk} \bar{\psi}^a \gamma_j \psi^b F_{0k}^{ab}$
0_S^{+-}	0^{+-} (exotic)	$a_1 \otimes B$	$\bar{\psi}^a \gamma_5 \gamma_i \psi^b \epsilon_{ijk} F_{jk}^{ab}$
0_P^{+-}	0^{+-} (exotic)	$a_1(\mathrm{P}) \otimes B$	$\bar{\psi}^b \gamma_j \overleftrightarrow{\partial}_k \psi^a F_{jk}^{ab}$
0_B^{+-}	0^{+-} (exotic)	J_B	$\bar{\psi}^a \gamma_0 \psi^a$
0_S^{--}	0^{--} (exotic)	$a_1 \otimes E$	$\bar{\psi}^a \gamma_5 \gamma_i \psi^b F_{i0}^{ab}$
0_P^{--}	0^{--} (exotic)	$a_1(\mathrm{P}) \otimes E$	$\epsilon_{ijk} \bar{\psi}^b \gamma_j \overleftrightarrow{\partial}_k \psi^a F_{0i}^{ab}$
1^{-+}	1^{-+} (exotic)	$\rho \otimes B$	$\bar{\psi}^a \gamma_j \psi^b F_{ji}^{ab}$
1_2^{-+}	1^{-+} (exotic)	$J_B \otimes E$	$\bar{\psi}^a \gamma_0 \psi^b F_{0i}^{ab}$
Q^4	1^{-+} (exotic)	$\pi \otimes a_1$	$\bar{\psi}_\alpha^a(\vec{x}) \gamma_5 \psi_\beta^a(\vec{x}) \bar{\psi}_\beta^b(\vec{y}) \gamma_5 \gamma_i \psi_\lambda^b(\vec{y})$

The remaining sections of Table I contain the operators with exotic quantum numbers. We have experimented with three 0^{+-} operators. The first two are formed from the a_1 quark bilinear and the color magnetic field, while the third is the J_B bilinear. Of these, the 0_P^{+-} source and sink gave the best signal. (The 0_P^{+-} operator in the form needed for the lattice computation is shown in the Appendix.)

There are two 0^{--} operators, using the ''pointlike'' and the ''P-wave'' a_1 bilinear, respectively, and the color electric field. Again, we found that the P-wave operator gave a better signal.

Finally, there are three 1^{-+} operators. The first is a quark and antiquark in a ''ρ'' state, with the color magnetic field. As is well known [10], a 1^{-+} hybrid can be constructed with the quark and antiquark in a relative S-wave state, and this is one of several arguments leading us to expect that it will be the lightest exotic hybrid. The second 1^{-+} operator is the charge bilinear $\bar{\psi}\gamma_0\psi$ combined with the color electric field. Of these two operators, we find that the first gives a better signal. The last operator is a four-quark operator. To use this operator as a source, we begin with the usual wall source, which is used as the source for a quark propagator computation. We then multiply the wall source by the pion operator (multiply by γ_5) and use this as the source for a computation of an antiquark propagator. The resulting propagator on the source time slice is then multiplied by the a_1 operator, (multiply by $\gamma_5\gamma_i$), and the result is used as the source for another antiquark propagator. Obviously this is expensive, since it involves an extra propagator computation. We have not used this operator as a ''sink'' operator, since to do this we would need a separate extra inversion at each time slice, instead of just at the source time slice. However, the ''crossed'' propagator with the four-quark operator as a source and the hybrid 1^{-+} operator as a sink turns out to be useful.

This work differs from the UKQCD study [6,7] in several ways. We used two different lattice spacings, $6/g^2=5.85$ and 6.15, with several κ values ranging from the strange to the charmed quark mass, while the UKQCD group used a single lattice spacing $6/g^2=6.0$ and a single κ value near the strange quark mass. The UKQCD lattices had a spatial size of about 1.6 fm, while we used lattices with a spatial size of about 2.2 fm. The spatial size of the lattice could be important if hybrids turn out to be large compared to ordinary mesons. We used the conventional Wilson action for the quark propagators, while the UKQCD group used the clover action, which reduces discretization effects in the quark propagators. The UKQCD group used 350 lattices with a single source point, while we used up to 30 lattices (depending on $6/g^2$ and κ), but with propagators from four wall sources on each lattice. The UKQCD group used the same operators for the source and sink. These operators were constructed from a quark at the source-sink point and an antiquark at fixed distances. In contrast, our sink operators have the quark and antiquark at the same point or, for the P-wave operators, at neighboring lattice points. Our source operators use a ''wall source'' in the Coulomb gauge, which amounts to using a quark source on all points of the source time slice, together with a sum over separations between the quark and antiquark. Coupled with the difference in quark-antiquark

separations in the hybrid operators is a difference in the way the field strength is computed. In the UKQCD work this is done by summing over different paths from the quark to the antiquark with appropriate signs, while we used $F_{\mu\nu}$ evaluated at a point. However, both groups ''fuzzed'' or ''smeared'' the gauge links in the operators, which also smears the distinction between the different $F_{\mu\nu}$. The UKQCD did try using hybrid operators with a ''pointlike'' $F_{\mu\nu}$ similar to those used here; however, they used local sources for the quark propagators, while we used wall sources. The UKQCD group found that these operators produced masses consistent with those from ''path sum'' hybrid operators. In fitting the propagators to extract masses, both groups combine information from different operators with the same quantum numbers and both include an excited state in the fits. Because there are several differences between the two groups' methods, it is impossible at this point to determine the effect of each difference on the statistical or systematic errors.

III. SIMULATION RESULTS

We used quenched lattices with the standard plaquette gauge action on $20^3\times48$ lattices at $6/g^2=5.85$ and on $32^3\times64$ lattices at $6/g^2=6.15$. These lattices were generated for quenched spectrum studies [11].

At $6/g^2=6.15$ we evaluated propagators at five values of the Wilson hopping parameter, with the largest one chosen at approximately the charm quark mass. We used π, ρ, a_1, and all of the exotic operators in Table I as source operators. For each source, we used all of the sink operators with the same quantum numbers, except for the Q^4 operator. For each lattice, we used four source time slices. For the lightest quark mass exotic propagators, we used 30 lattices, with fewer lattices for the smaller κ values. Because we do not need as many lattices to get good values for the π and ρ masses, and because we did not implement the Q^4 source until the project was already started, we do not have all the propagators on all of the lattices.

At $6/g^2=5.85$ we evaluated propagators with π, ρ, $a_1(\mathrm{P})$, 1^{-+}, and Q^4 sources. Since our previous work on $6/g^2=5.6$ two-flavor lattices and our concurrent work at $6/g^2=6.15$ had found the 1^{-+} to be the lightest of the exotics and the one for which we had the best signals, we did not do the 0^{+-} and 0^{--} propagators on the $6/g^2=5.85$ lattices. We used 23 lattices, with four source time slices on each lattice.

Since propagators with different values of κ were computed on the same quenched lattices, the mass estimates are strongly correlated. Also, there is the possibility of correlations among the propagators with different source time slices on the same lattice, which we have ignored in computing the covariance matrix. On the other hand, the different lattices are uncorrelated, unlike the situation in most full QCD calculations. To account for these correlations, especially when extrapolating or interpolating masses to different κ values, a jackknife analysis is useful. At $6/g^2=5.85$ all of the propagators were run on the same set of lattices. There we used a single-elimination jackknife, in which mass fits to the selected distance range and the extrapolation to κ_c were repeated, each time omitting one lattice. For the mass estimates at $6/g^2=5.85$ in Table II the first parenthesized error esti-

TABLE II. Mass estimates for ordinary $\bar{q}q$ mesons. The a_1 mass estimates used the $a_1(P)$ source and sink. An asterisk indicates a point from a 12^3 lattice. Where present, a second parenthesized error is a jackknife estimate. Fits at $\kappa = 0.154$ for $6/g^2 = 6.15$ are jackknife extrapolations to κ_c.

$6/g^2$	Particle	κ	Fit range	χ^2/N_{DF}	Mass
6.15	π	0.1350	21–25	1.7/3	1.0967(45)(56)
		0.1450	18–24	1.5/5	0.6583(7)(8)
		0.1480	18–24	0.3/5	0.5117(7)(7)
		0.1500	18–24	1.4/5	0.4042(8)(5)
		0.1520	18–24	6.4/5	0.2788(10)(3)
6.15	ρ	0.1350	21–25	2.4/3	1.1067(5)(8)
		0.1450	18–24	4.4/5	0.6850(10)(15)
		0.1480	18–24	2.2/5	0.5518(13)(17)
		0.1500	18–24	2.4/5	0.4591(17)(14)
		0.1520	18–24	2.1/5	0.3644(34)(48)
		0.154	extrap.	—	0.2738(-)(42)
6.15	a_1	0.1350	16–20	2.6/3	1.274(8)(10)
		0.1450	8–14	9.0/5	0.858(5)(5)
		0.1480	8–14	8.5/5	0.741(6)(5)
		0.1500	8–14	7.4/5	0.658(6)(5)
		0.1520	8–14	4.1/5	0.581(10)(6)
		0.154	extrap.	—	0.505(-)(7)
5.85	π	0.1450	13–18	1.0/4	0.990(1)(1)
		0.1500	13–18	1.6/4	0.788(1)(1)
		0.1525	13–18	1.8/4	0.681(1)(1)
		0.1540*	5–8	17.4/24	0.610(2)
		0.1550	13–18	2.4/4	0.566(1)(1)
		0.1570*	5–18	17.9/24	0.458(4)
		0.1590*	5–18	15.3/24	0.332(6)
5.85	ρ	0.1450	13–18	2.8/4	1.023(1)(2)
		0.1500	13–18	2.2/4	0.841(2)(2)
		0.1525	13–18	2.1/4	0.751(2)(2)
		0.1540*	8–19	5.4/10	0.693(5)
		0.1550	13–18	2.3/4	0.660(3)(3)
		0.1570*	8–19	5.6/10	0.579(8)
		0.1590*	8–19	3.7/10	0.499(17)
5.85	a_1	0.1450	6–11	1.7/4	1.312(8)(8)
		0.1500	6–11	3.0/4	1.153(10)(9)
		0.1525	6–11	4.5/4	1.077(12)(10)
		0.1550	6–11	5.5/4	1.005(14)(13)

mate is from the covariance matrix, and the second is from the jackknife analysis. These two estimates agree well. At $6/g^2 = 6.15$ we do not have all the propagators or all the κ values on every lattice. Therefore we divided the lattices up into five jackknife blocks, with each block containing about the same number of each kind of propagator, and ran the fits for the selected distance ranges, each time omitting one fifth of the lattices. Again, when there is a second parenthesized error estimate in Table II it is from the jackknife analysis.

We first need an estimate of the lattice spacing. This can be done by extrapolating the ρ mass to the physical quark mass, or essentially to κ_c, or from the $1S$-$1P$ mass splitting for heavy quarks. Table II contains mass estimates for the pseudoscalar, vector, and 1^{++} $\bar{q}q$ ("π," "ρ," and "a_1")

states. These mass estimates are crude by today's standards, but we need them only for approximately determining the lattice spacing. For $6/g^2 = 5.85$ we include π and ρ mass estimates at additional κ values, done on a 12^3 spatial lattice, coming from our f_B calculations [12].

At $6/g^2 = 5.85$ we estimate $1/\kappa_c = 6.205(3)$ from extrapolating the squared pion masses from the largest four κ values. If we estimate the lattice spacing by extrapolating the ρ mass to κ_c, we find $a^{-1} = 1.80(6)$ GeV or 2.00(11) GeV, depending on whether m_ρ or m_ρ^2 is extrapolated linearly in $1/\kappa$. These extrapolations are plotted in Fig. 3.

At $6/g^2 = 6.15$ we do not have the luxury of extra pion masses near κ_c. A linear fit of m_π^2 in $1/\kappa$ does not work well, and so we fit the pion mass at the four largest κ's to a
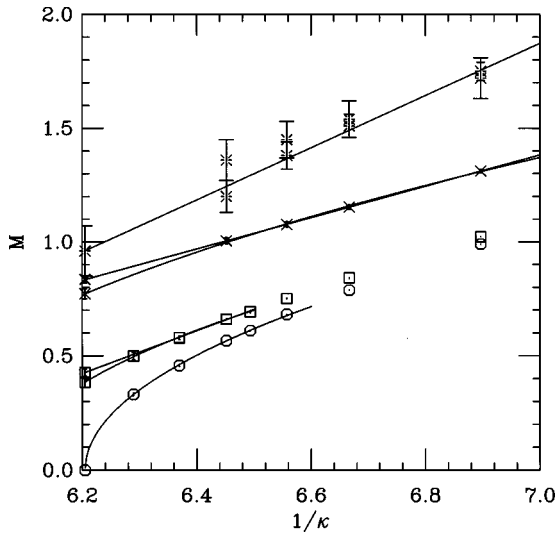
FIG. 3. Particle masses at $6/g^2 = 5.85$ and extrapolations to κ_c^{-1}. The octagons are pion masses, and the line is a fit to m_π^2 linear in $1/\kappa$. Squares and crosses are ρ and a_1 masses, respectively. For the ρ and a_1 we show two extrapolations of the mass to κ_c, one with m_{ρ,a_1} linear in $1/\kappa$ and the other with m_{ρ,a_1}^2 linear in $1/\kappa$. Finally, the bursts are the 1^{-+} exotic meson. We show two fits of the 1^{-+} meson for each κ. The lower one uses the two-source, two-mass fits as illustrated in Fig. 7, while the upper one uses only the $1^{-+} \to 1^{-+}$ propagator.

quadratic in $1/\kappa$ to estimate $1/\kappa_c = 6.4895(10)$. This fit had a χ^2 of 0.5 with one degree of freedom. An extrapolation of m_ρ to this κ_c gives $am_\rho(\kappa_c) = 0.274(4)$ or $a^{-1} = 2.81(4)$ GeV, where the error is a jackknife estimate. These extrapolations are plotted in Fig. 4. Another possibility, following the Fermilab group, is to use the splitting between the average S-wave charmonium masses and the P-wave masses to
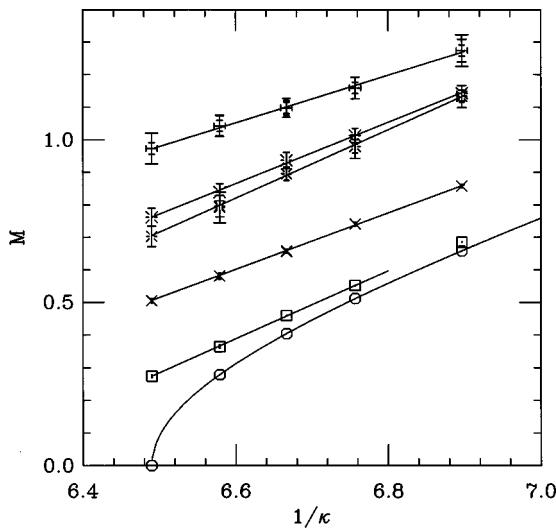

FIG. 4. Particle masses at $6/g^2 = 6.15$ and extrapolations to κ_c^{-1}. The symbols are the same as in Fig. 3, and the fancy pluses are a 0^{+-} exotic. Here the pion mass is fit to a quadratic in $1/\kappa$. Again we show two fits of the 1^{-+} meson for each κ, the lower one fitting both source operators simultaneously and the upper one fitting only the $1^{-+} \to 1^{-+}$ propagator. The $\kappa = 0.1350$ or $1/\kappa = 7.407$ charmonium point is not in the range shown here.
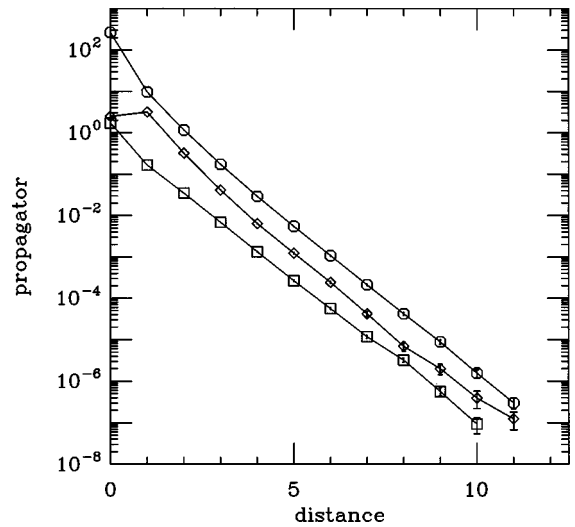

FIG. 5. Propagators for the 1^{-+} exotic meson at $6/g^2 = 6.15$ and $\kappa = 0.1350$. The octagons are for a 1^{-+} source and sink, the diamonds for a 1^{-+} source with a 1_2^{-+} sink, and the squares for a Q^4 source with a 1^{-+} sink.

estimate the lattice spacing. At $\kappa = 0.1350$, using the 1^{++} meson as the P-wave mass and $\frac{3}{4}m_{1^{--}} + \frac{1}{4}m_{0^{-+}}$ as the S-wave mass, with 457 MeV as the experimental value for charmonium, we get $a^{-1} = 2.85(1)$ GeV.

Figure 5 shows exotic propagators at $6/g^2 = 6.15$ and $\kappa = 0.1350$. For the 1^{-+} exotic we show three propagators. One has the 1^{-+} operator as its source and sink, the second the 1^{-+} operator as the source and the 1_2^{-+} operator as the sink, and the third has the Q^4 operator as its source and the 1^{-+} operator as its sink. Figure 6 is a similar figure for our smallest quark mass, $\kappa = 0.1520$, except that instead of the $1^{-+} \to 1_2^{-+}$ propagator we have a $1_2^{-+} \to 1_2^{-+}$ propagator. Compared to the propagators for conventional mesons, these exotic propagators are quite noisy, and we must use fairly
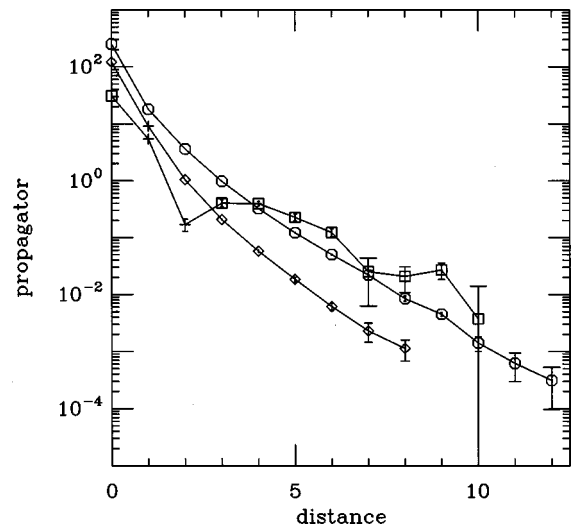

FIG. 6. Propagators for the 1^{-+} exotic meson at $6/g^2 = 6.15$ and $\kappa = 0.1520$. The octagons are for a 1^{-+} source and sink, the diamonds for a 1_2^{-+} source and sink, and the squares for a Q^4 source with a 1^{-+} sink. Pluses indicate the absolute value of a propagator that changes sign with increasing distance.
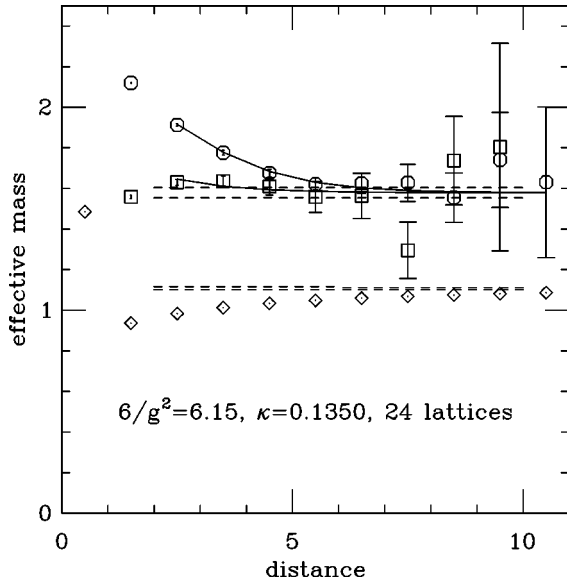
FIG. 7. Effective masses for the ρ and 1^{-+} exotic at $6/g^2=6.15$ and $\kappa=0.1350$, approximately the charm quark mass. The octagons are the effective mass from propagators with the 1^{-+} operator as both source and sink, and the squares are the effective mass with the Q^4 source and 1^{-+} sink. These propagators were fit with two source amplitudes and two masses as described in the text, over the distance range 2–11. The solid lines near the plot symbols are the effective masses reconstructed from the fit. The upper pair of horizontal lines indicates the $\pm 1\sigma$ range for the ground state mass in this fit. The diamonds are the ρ (more accurately, the ψ) effective mass. The horizontal bars near the diamonds are the $\pm 1\sigma$ limits on the ground state mass from fits to the ρ propagator. The lines running from $d=2$ to 6 are a two-mass fit to the propagator over this range, while the closely spaced lines for $d>6$ are from a single-exponential fit over distance range 21 to 25.

FIG. 8. Effective masses for the 1^{-+} meson at $6/g^2=6.15$ and $\kappa=0.1520$, approximately the strange quark mass. The symbols and lines have the same meaning as in Fig. 7. These effective masses correspond to the propagators in Fig. 6.

short distances for the mass fits. As seen in Figs. 5 and 6, this problem becomes worse as the quark mass is made lighter. In fact, these exotic propagators fall below their statistical error at a distance smaller than the minimum distance we use for a single mass fit for the π or ρ. This means that contamination by excited states might be a serious problem. We have therefore done fits to two exponentials for the exotic states. We can do this only over a small range of minimum distance. In particular, if we take the minimum distance to be too large, we get fits with a very large excited state mass, which is essentially just a δ function removing the shortest distance point from the fit and giving the same result as a one mass fit with a minimum distance one unit larger. Of course, we reject such fits since they are basically one mass fits.

In these fits, we would like to use information from the different source and sink operators, by simultaneously fitting to two or more combinations of operators with different amplitudes for each source and sink but the same masses for all of them:

$$\langle \mathcal{O}_i(0)\mathcal{O}_j(t)\rangle = A_i^0 A_j^0 e^{-m_0 t} + A_i^1 A_j^1 e^{-m_1 t} + \cdots, \quad (1)$$

where i and j label the source and sink operators, respectively, and m_0 and m_1 are the ground state and excited state masses. For this to be useful, the relative overlaps of the different operators with the ground state and excited state
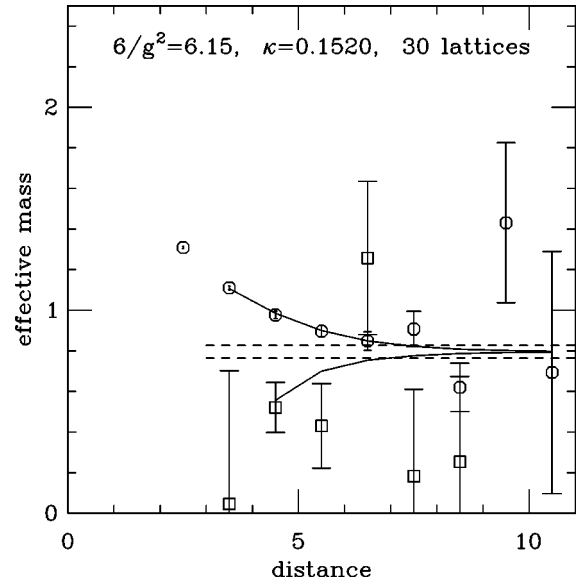
should be as different as possible. For the 1^{-+} propagators it turns out that the 1^{-+} and 1_2^{-+} operators have essentially the same effective masses. Since the propagators with 1_2^{-+} operators are noisier than those with 1^{-+} source and sink, including these propagators in the fitting did not help (any gain in statistics was not worth the extra degrees of freedom in the fitting). However, the correlator generated from the Q^4 source, which we introduced to investigate coupling to four quark states, does have an effective mass at short distance significantly different from that generated from the hybrid 1^{-+} source. This can be seen in Fig. 7, which shows the effective masses corresponding to the $1^{-+}\rightarrow 1^{-+}$ and $Q^4\rightarrow 1^{-+}$ propagators at our heaviest quark mass, $\kappa=0.1350$, and in Fig. 8 which shows the effective masses at our lightest quark mass, $\kappa=0.1520$, corresponding to the propagators in Fig. 6. As might be expected from this, simultaneously fitting the 1^{-+} and Q^4 source propagators, each with the 1^{-+} sink operator, to two masses gave the best mass estimates. The ground state mass from this fit and the effective masses from the fit are also shown in Figs. 7 and 8. Of course, this two-source fit makes the assumption that the excited state (or combined effect of many excited states treated as a single state in the fitting program) is the same in both propagators. Therefore we tabulate results both from the simultaneous fits to two source operators and from fits using only the 1^{-+} source operator. In the cases of the 0^{+-} and 0^{--} propagators, we have not investigated four-quark source operators. For the 0^{+-} and 0^{--} hybrid operators, the P-wave source and sink operators generally gave the best statistical errors, and so were the only ones we fit.

One might still worry that we are not extracting the correct ground state masses from such short distances. As a partial check, we take the ρ propagator, for which a quite convincing plateau in the effective mass is seen at larger distances, and make a two-mass fit to this propagator at the same distances we use for the hybrid fits. (Since the hybrid
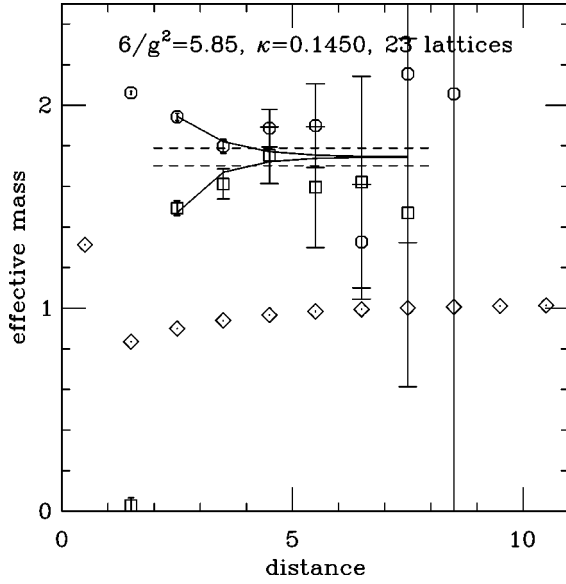
FIG. 9. Effective masses for the 1^{-+} meson and the ρ at $6/g^2=5.85$ and $\kappa=0.1450$. The symbols and lines have the same meaning as in Fig. 7.
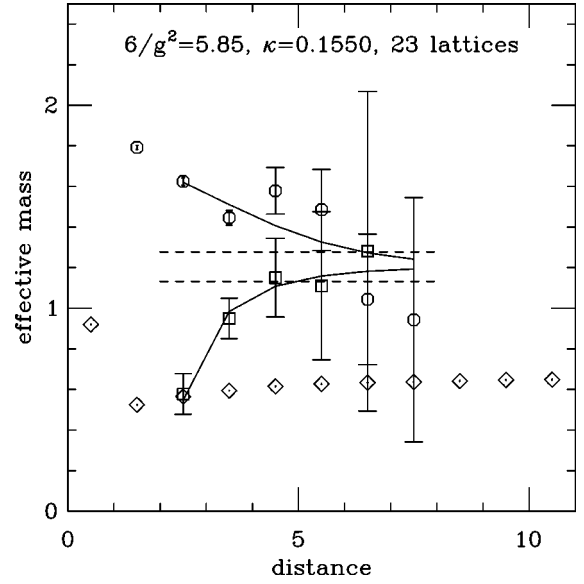

FIG. 10. Effective masses for the 1^{-+} meson and the ρ at $6/g^2=5.85$ and $\kappa=0.1550$. The symbols and lines have the same meaning as in Fig. 7.

fits are dominated by the more accurate points at the smaller distances in the fitting range, we fit the ρ mass to the smaller distances in the range.) In this case, at $6/g^2=6.15$ and $\kappa=0.1350$, which is the charm quark mass, we find that the ρ (more accurately, the J/ψ) mass from a single-exponential fit to distance range 21–25 is 1.1067(5) ($\chi^2/d=2.4/3$), while a two-mass fit over distance range 2–6 gives a ground state mass 1.109(8) with an excited state mass of 1.264(21) ($\chi^2/d=1.5/1$), in excellent agreement with the single-exponential fit from long distances. The ρ (J/ψ) effective mass and these fits are also shown in Fig. 7. While this result is encouraging, we should caution the reader that the number

of excited states and the mass gap between the ground and excited states might be very different for the ρ meson and the exotic mesons.

Another important test is to verify that the mass estimates are independent of the fitting range used. Here we are not in as good a position, since we generally have only two or three minimum distances where we can get a two mass fit with reasonable χ^2. However, within the fairly poor statistical errors, the exotic mass estimates are generally consistent among these fits.

The $6/g^2=5.85$ fits to the 1^{-+} are done in similar fashion. In Figs. 9 and 10 we show the effective masses and the

TABLE III. Mass estimates for the exotic 1^{-+} meson for $6/g^2=5.85$. Where two-source operators are listed, a simultaneous fit was done to propagators from both sources, with the masses forced to be the same for each source. Where two masses were used in the fit, the last column shows the excited state mass produced by the fit. Where present, a second parenthesized error is a jackknife estimate.

κ	Source(s)$\rightarrow$sink	Masses	Fit range	χ^2/N_{DF}	Mass	M^*
0.1450	$1^{-+}\rightarrow1^{-+}$	1	3–9	3.9/5	1.81(3)	
	$1^{-+}\rightarrow1^{-+}$	1	4–10	3.5/5	1.88(8)	
	$Q^4\rightarrow1^{-+}$	1	3–7	0.7/3	1.65(5)	
	$1^{-+}\rightarrow1^{-+}$	2	1–9	7.3/5	1.72(9)	2.45(19)
	$Q^4,1^{-+}\rightarrow1^{-+}$	2	1–8	9.1/10	1.71(3)	2.42(6)
	$Q^4,1^{-+}\rightarrow1^{-+}$	2	2–8	6.6/8	1.75(4)(5)	2.86(44)
0.1500	$1^{-+}\rightarrow1^{-+}$	2	1–9	5.8/5	1.54(8)	2.33(19)
	$Q^4,1^{-+}\rightarrow1^{-+}$	2	1–8	7.4/10	1.47(3)	2.20(4)
	$Q^4,1^{-+}\rightarrow1^{-+}$	2	2–8	6.2/8	1.51(5)(6)	2.31(21)
0.1525	$1^{-+}\rightarrow1^{-+}$	2	1–9	5.2/5	1.45(8)	2.28(18)
	$Q^4,1^{-+}\rightarrow1^{-+}$	2	1–8	7.4/10	1.33(3)	2.10(4)
	$Q^4,1^{-+}\rightarrow1^{-+}$	2	2–8	6.0/8	1.38(6)(7)	2.08(15)
0.1550	$1^{-+}\rightarrow1^{-+}$	2	1–9	5.0/5	1.36(9)	2.22(17)
	$Q^4,1^{-+}\rightarrow1^{-+}$	2	1–8	9.3/10	1.19(4)	2.00(3)
	$Q^4,1^{-+}\rightarrow1^{-+}$	2	2–8	6.0/8	1.20(7)(8)	1.88(10)

TABLE IV. Mass estimates for the exotic 1^{-+} meson for $6/g^2 = 6.15$. The format is the same as Table III. The final line is an extrapolation to κ_c^{-1}, using the distance range 3–11 for the four largest κ values.

κ	Source(s)→sink	Masses	Fit range	χ^2/N_{DF}	Mass	M^*
0.1350	$1^{-+} \to 1^{-+}$	2	1–11	2.3/7	1.61(2)	2.52(4)
	$1^{-+} \to 1^{-+}$	2	2–11	1.3/6	1.58(3)	2.42(11)
	$1^{-+} \to 1^{-+}$	2	3–11	1.2/5	1.59(4)	2.54(42)
	$Q^4, 1^{-+} \to 1^{-+}$	2	1–11	18.1/16	1.63(1)	2.57(3)
	$Q^4, 1^{-+} \to 1^{-+}$	2	2–11	6.8/14	1.58(3)	2.38(9)
	$Q^4, 1^{-+} \to 1^{-+}$	2	3–11	6.5/12	1.57(4)	2.28(23)
0.1450	$1^{-+} \to 1^{-+}$	2	1–11	11.5/7	1.189(16)	2.19(4)
	$1^{-+} \to 1^{-+}$	2	2–11	4.5/6	1.143(24)	2.24(7)
	$Q^4, 1^{-+} \to 1^{-+}$	2	2–11	15.2/14	1.109(16)	1.90(4)
	$Q^4, 1^{-+} \to 1^{-+}$	2	3–11	8.8/12	1.134(19)(34)	2.04(18)
	$Q^4, 1^{-+} \to 1^{-+}$	2	4–11	4.2/10	1.161(39)	1.62(47)
0.1480	$1^{-+} \to 1^{-+}$	2	2–11	4.8/6	1.013(22)	2.16(6)
	$1^{-+} \to 1^{-+}$	2	3–11	3.0/5	1.039(25)	2.30(43)
	$Q^4, 1^{-+} \to 1^{-+}$	2	2–11	30.4/14	0.955(15)	1.76(4)
	$Q^4, 1^{-+} \to 1^{-+}$	2	3–11	15.1/12	0.980(21)(36)	1.74(12)
	$Q^4, 1^{-+} \to 1^{-+}$	2	4–11	6.3/10	1.019(29)	1.67(33)
0.1500	$1^{-+} \to 1^{-+}$	2	2–11	8.8/6	0.937(24)	2.16(6)
	$1^{-+} \to 1^{-+}$	2	3–11	8.7/5	0.943(29)	1.91(24)
	$Q^4, 1^{-+} \to 1^{-+}$	2	2–11	48.9/14	0.868(17)	1.70(03)
	$Q^4, 1^{-+} \to 1^{-+}$	2	3–11	22.7/12	0.897(22)(19)	1.63(10)
	$Q^4, 1^{-+} \to 1^{-+}$	2	4–11	15.5/10	0.943(26)	1.88(42)
0.1520	$1^{-+} \to 1^{-+}$	2	2–11	6.9/6	0.839(26)	2.13(6)
	$1^{-+} \to 1^{-+}$	2	3–11	6.4/5	0.820(37)	1.63(16)
	$Q^4, 1^{-+} \to 1^{-+}$	2	2–11	38.7/14	0.789(23)	1.66(4)
	$Q^4, 1^{-+} \to 1^{-+}$	2	3–11	16.0/12	0.796(33)(47)	1.54(11)
	$Q^4, 1^{-+} \to 1^{-+}$	2	4–11	14.3/10	0.827(40)	1.76(50)
0.154	$Q^4, 1^{-+} \to 1^{-+}$	2	extrap.	—	0.705(na)(32)	

fits to the propagators for our largest and smallest κ values, $\kappa = 0.1450$ and 0.1550, at $6/g^2 = 5.85$.

Tables III and IV contain selected mass fits for the 1^{-+} mesons at $6/g^2 = 5.85$ and 6.15, respectively. When two masses were used in the fit, both the ground state and the excited state mass are tabulated. However, this excited state mass is almost certainly some sort of weighted average of many states and should not be taken seriously as a mass estimate.

Finally, Table V contains selected fits for the 0^{+-} exotic at $6/g^2 = 6.15$. This particle is clearly heavier than the 1^{-+}, and our estimates for its mass are worse. This is partly because we have only the one-source operator for this meson and partly because (nonrelativistically) the quark and antiquark are in a relative P-wave state, and we were led to use a more complicated source operator.

We were unable to get credible mass estimates from the 0^{--} propagators, suggesting that this state, if it exists at all, is even heavier than the 1^{-+} and 0^{+-}.

IV. DISCUSSION AND CONCLUSIONS

In this concluding section we discuss the conversion of our mass estimates from lattice units to physical mass units,

estimate systematic errors, and describe briefly the observational status of 1^{-+} exotic hadrons.

Figures 3 and 4 collect and display our results for nonexotic mesons and for the 1^{-+} and the 0^{+-} exotic mesons. We also show extrapolations to κ_c, where the error on the extrapolations comes from the jackknife analysis. For the 1^{-+} hybrid we plot fits to both the one-source operator and two-source operator mass estimates. The difference between these fits is an indication of the possible systematic error from excited states in the propagators. While this difference is small for the charmonium point, at the strange quark mass for $6/g^2 = 6.15$ it amounts to 117 MeV and when extrapolated to κ_c becomes 165 MeV.

One of the known problems with the Wilson quark action is that it consistently underestimates spin splittings of hadrons [13]. This suggests that the average mass of the S-wave mesons might be a better mass standard than the ρ mass alone. (We have already used this logic in Sec. III when we used the splitting between the P-wave and the average S-wave charmonium mass as a length scale.) In Fig. 11 we plot the ratio of the 1^{++} P-wave meson (a_1) to the average S-wave meson mass, $\frac{3}{4}m_{1^{--}} + \frac{1}{4}m_{0^{-+}}$. For the horizontal scale we use the average S-wave mass divided by the aver-

TABLE V. Mass estimates for the exotic 0^{+-} meson for $6/g^2 = 6.15$. The format is the same as Table III.

κ	Source(s)→sink	Masses	Fit range	χ^2/N_{DF}	Mass	M^*
0.1350	$0_P^{+-} \to 0_P^{+-}$	1	5–9	3.6/3	1.72(2)	
	$0_P^{+-} \to 0_P^{+-}$	1	6–10	2.7/3	1.69(3)	
	$0_P^{+-} \to 0_P^{+-}$	1	7–11	1.2/3	1.63(5)	
	$0_P^{+-} \to 0_P^{+-}$	2	2–11	4.5/6	1.66(3)(5)	2.52(6)
0.1450	$0_P^{+-} \to 0_P^{+-}$	1	5–9	2.9/3	1.32(3)	
	$0_P^{+-} \to 0_P^{+-}$	1	6–10	3.6/3	1.30(4)	
	$0_P^{+-} \to 0_P^{+-}$	1	7–11	2.7/3	1.23(7)	
	$0_P^{+-} \to 0_P^{+-}$	2	2–11	3.9/6	1.27(4)(5)	2.24(7)
0.1480	$0_P^{+-} \to 0_P^{+-}$	1	5–9	1.9/3	1.20(2)	
	$0_P^{+-} \to 0_P^{+-}$	1	6–10	2.2/3	1.18(4)	
	$0_P^{+-} \to 0_P^{+-}$	1	7–11	1.9/3	1.11(8)	
	$0_P^{+-} \to 0_P^{+-}$	2	2–11	3.5/6	1.16(3)(3)	2.16(6)
0.1500	$0_P^{+-} \to 0_P^{+-}$	1	5–9	0.7/3	1.13(2)	
	$0_P^{+-} \to 0_P^{+-}$	1	6–10	5.4/3	1.08(4)	
	$0_P^{+-} \to 0_P^{+-}$	1	7–11	4.9/3	1.01(9)	
	$0_P^{+-} \to 0_P^{+-}$	2	2–11	7.5/6	1.10(3)(2)	2.16(6)
0.1520	$0_P^{+-} \to 0_P^{+-}$	1	5–9	2.7/3	1.08(3)	
	$0_P^{+-} \to 0_P^{+-}$	1	6–10	1.9/3	0.98(6)	
	$0_P^{+-} \to 0_P^{+-}$	1	7–11	1.7/3	0.94(13)	
	$0_P^{+-} \to 0_P^{+-}$	2	2–11	4.2/6	1.04(3)(3)	2.13(7)

age S-wave mass at the physical point, where $m_\pi/m_\rho = 0.18$. In other words, the units of the horizontal axis are $\frac{3}{4}m_\rho + \frac{1}{4}m_\pi = 610$ MeV. The vertical scale is the ratio of the P-wave 1^{++} meson mass or the 1^{-+} exotic meson mass to the S-wave mass. The vertical lines indicate the strange quark and charmonium points. In locating the strange quark line, we have followed the UKQCD procedure of using an
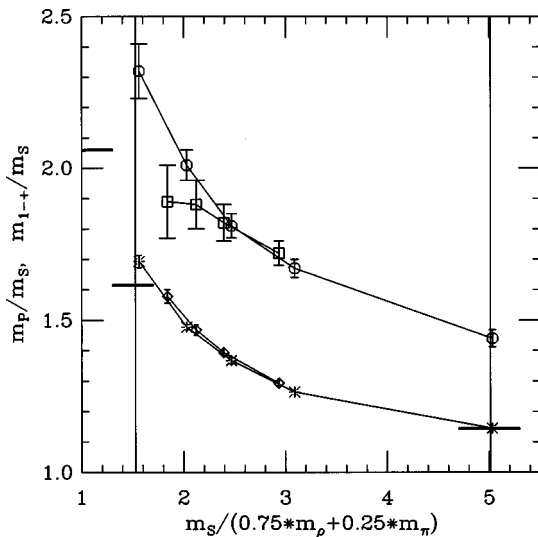

FIG. 11. Ratios of the 1^{++} (P-wave) meson mass and the 1^{-+} exotic mass to the average S-wave meson mass. Diamonds and bursts are the 1^{++} at $6/g^2 = 5.85$ and 6.15, respectively, and squares and octagons are the 1^{-+} at 5.85 and 6.15, respectively. The horizontal and vertical scales and the vertical and horizontal lines are described in the text.

''unmixed'' η_{strange} mass of 680 MeV [7]. By definition, the light quark point is the left-hand side of the graph. Where they intersect the left side of the graph and the two vertical lines, the three bold horizontal lines indicate the experimental values of the 1^{++} meson mass divided by the S-wave mass for light quarks, strange quarks, and charm quarks, respectively.

A nice feature of this graph is the good agreement of the P-wave masses between the $6/g^2 = 5.85$ and 6.15 lattices. For heavy quarks the agreement of the 1^{-+} exotic is equally good, but there is some difference for the light quarks. We suspect that the $6/g^2 = 5.85$ points are incorrect here. In Fig. 10 we see that the 1^{-+} fit at $6/g^2 = 5.85$ and $\kappa = 0.1550$ is questionable at best, and Fig. 3 or Table III shows that had we used the one-source fits for this point we would have obtained a 13% larger mass. The exact agreement between our predicted and the observed charmonium mass is undoubtedly fortuitous, but this agreement and the trend toward agreement between the 5.85 and 6.15 estimates at larger quark mass encourages us to quote a charmed hybrid meson mass with suitable caveats.

Using this average S-wave mass as the length scale for the charmonium exotics gives an *uncorrected* mass of 4390(80) MeV for the 1^{-+} and 4610(110) MeV for the 0^{+-}. We emphasize that these quoted errors are statistical only and do not take into account contamination from excited states in the chosen fitting ranges, or discretization errors in the gauge and quark action, or effects of the quenched approximation. As mentioned above, the errors from excited state contamination, which can be crudely estimated by looking at how the estimated mass varies as a function of minimum distance in the fit or whether the second source opera-

TABLE VI. Predictions for the mass of the light and charmonium 1^{-+} states from various approaches to QCD, obtained from [3].

Mass (GeV)	Method
Light quark 1^{-+} mass	
$1.3 \rightarrow 1.8$	Bag model
$1.8 \rightarrow 2.0$	Flux-tube model
$1.8 \rightarrow 1.9$	Flux-tube model of Barnes $et\ al.$ [3]
$2.1 \rightarrow 2.5$	QCD sum rules (mostly after 1984)
$1.97(9_{\text{stat.}})(30_{\text{lattice}})(??_{\text{quench}})$	This work
Charmonium 1^{-+} mass	
≈ 3.9	Adiabatic bag model
$4.2 \rightarrow 4.5$	Flux-tube model
$4.1 \rightarrow 4.2$	Flux-tube model of Barnes $et\ al.$ [3]
$4.19 \pm$ syst.	Heavy quark lattice gauge theory [4]
$4.1 \rightarrow 5.3$	QCD sum rules (mostly after 1984)
$4.39(8_{\text{stat.}})(20_{\text{lattice}})(??_{\text{quench}})$	This work

tor is included, are probably about the same size as the statistical errors. The close agreement of the 1^{++} masses and the 1^{-+} masses for heavier quarks in Fig. 11 suggests that errors from the nonzero lattice spacing might be small. However, we also note that in our studies of charmed pseudoscalar meson decay constants we find a discretization error in the decay constants of 10%–15% at $6/g^2 = 6.15$ [14]. It might be that decay constants are more sensitive to lattice spacing errors than mass, since the decay constants are basically wave functions at the origin and are strongly affected by the coarseness of the lattice at short distance. Although it is little better than a guess, we propose using 15% of the splitting between the hybrid state and the $\bar{c}c$ states, or 200 MeV, as an estimate of the systematic error from both excited state contamination and lattice artifacts. The largest systematic error probably comes from using the quenched approximation, and this is the hardest error to estimate. It will surely be large, since, as discussed in the Introduction, these hybrid states can mix with four-quark states. In this work we looked at mixing with states containing four heavy quarks, but in the real world the important four-quark states would contain the charmed quark and antiquark and a light sea quark and antiquark. This charmonium 1^{-+} is quite far above the $D\bar{D}$ threshold. Because of the remaining systematic uncertainties, it is not clear whether it is above the S-wave + P-wave $D\bar{D}$ threshold, which in many model calculations determines whether its decay width is large [15,3].

At the strange quark mass (our largest κ at $6/g^2 = 6.15$), we estimate the mass of the 1^{-+} hybrid to be $2170 \pm 80 \pm$ systematic MeV. As noted at the beginning of this section, the systematic error from excited state contamination is on the order of 100 MeV, and the error from nonzero lattice spacing is probably as large or larger. Considering the large errors, this estimate is consistent with the mass quoted by the UKQCD Collaboration, 2000(200) MeV [7].

If we take seriously the extrapolation of the 1^{-+} mass to light quarks in Fig. 4, we get a mass of 1970(90) MeV for the light quark exotic hybrid, again with large systematic errors. Considering the lack of agreement in the 1^{-+} mass estimates at $6/g^2 = 5.85$ and 6.15 at light quark mass and the

effects of extrapolating in κ, we use 300 MeV as an estimate of the error on this number from lattice artifacts.

We briefly review the observational evidence relevant to our results. The particle data table [16] does not list any confirmed 1^{-+} hybrid meson states. However, a number of potential candidates are mentioned. There is some evidence for a 1^{-+} hybrid state with a mass of around 1.4 GeV and another with a mass around 1.9 GeV. The original evidence for a 1^{-+} state at 1.4 GeV found by the GAMES Collaboration [17] was criticized in [18]. However, recent work by the E852 Collaboration [19] reports evidence for a 1^{-+} hybrid state with a mass of $1370 \pm 16^{+50}_{-30}$ MeV. This paper [19] also lists other experiments that have reported a low mass for the 1^{-+} state. Our result favors a hybrid assignment for states around 1.9 GeV [20,21]. However, we stress that more simulations are required to quantify and reduce the systematic errors in our results before definitive results for the mass of the 1^{-+} state can be obtained from quenched lattice QCD.

In Table VI (obtained from [3]) we collect results for the mass of the light 1^{-+} hybrid obtained from a variety of models. We note that our prediction for the mass of the 1^{-+} state is consistent with the flux-tube estimate. Only the bag model calculation obtains a mass close to the E852 experimental result.

Unfortunately, no good candidates for the theoretically expected 1^{-+} hybrid charmonium state have been observed [16]. Such a state is also expected in flux-tube models, which are most plausible for heavy quark systems and furthermore provide information about branching ratios. Table VI also contains some predictions (taken from [3]) for the mass of the 1^{-+} state in the charmonium system.

Although we have concentrated on exotic hybrids in this work, lattice methods, particularly with dynamical quark loops included, could also address interesting issues regarding nonexotic states. For example, Close and Page characterize the $\psi(4040)$ and $\psi(4160)$ states as mixtures of $\bar{c}c$ and $\bar{c}cg$ [22]. Close proposes that hybrid states could help explain the "anomalous" production of charmonium observed by the Collider Detector at Fermilab (CDF) group [23]. In

both cases the occurrence of a nonexotic hybrid state in the range 4–4.3 GeV is essential.

Future efforts in lattice calculations of exotic hybrids should be directed at reducing the variety of systematic errors, including finite lattice spacing, excited state contamination, and the effects of quenching. Particularly important is to understand the extent of mixing with four-quark states.

APPENDIX

Here we write the 0^{+-} P-wave operator 0_P^{+-} in the form needed for the lattice computation. We are interested in zero spatial momentum, and so we are summing over spatial coordinates and can freely translate the summation variable. We wish to write the operator as $\bar{\psi}(\vec{x})$ times a sum of fields at $\vec{x}$ and neighboring points. In these expressions, it is understood that fields at neighboring points must be parallel transported to $\vec{x}$, so that $\bar{\psi}(\vec{x})\psi(\vec{x}+\hat{k})$ means $\bar{\psi}(\vec{x})U_k(\vec{x})\psi(\vec{x}+\hat{k})$:

$$
\begin{aligned}
\mathcal{O}_P^{+-} &= \sum_x \sum_{jk} \bar{\psi}^b \gamma_j (\vec{\partial}_k - \overleftarrow{\partial}_k) \psi^a F_{jk}^{ab} = \sum_x \sum_{jk} \bar{\psi}^b(\vec{x}) \gamma_j \psi^a(\vec{x}+\hat{k}) F_{jk}^{ab}(\vec{x}) - \bar{\psi}^b(\vec{x}) \gamma_j \psi^a(\vec{x}-\hat{k}) F_{jk}^{ab}(\vec{x}) \\
&\quad - \bar{\psi}^b(\vec{x}+\hat{k}) \gamma_j \psi^a(\vec{x}) F_{jk}^{ab}(\vec{x}) + \bar{\psi}^b(\vec{x}-\hat{k}) \gamma_j \psi^a(\vec{x}) F_{jk}^{ab}(\vec{x}) \\
&= \sum_x \sum_{jk} \bar{\psi}^b(\vec{x}) \gamma_j \psi^a(\vec{x}+\hat{k}) F_{jk}^{ab}(\vec{x}) - \bar{\psi}^b(\vec{x}) \gamma_j \psi^a(\vec{x}-\hat{k}) F_{jk}^{ab}(\vec{x}) \\
&\quad - \bar{\psi}^b(\vec{x}) \gamma_j \psi^a(\vec{x}-\hat{k}) F_{jk}^{ab}(\vec{x}-\hat{k}) + \bar{\psi}^b(\vec{x}) \gamma_j \psi^a(\vec{x}+\hat{k}) F_{jk}^{ab}(\vec{x}+\hat{k}) \\
&= \sum_x \sum_{jk} \bar{\psi}^b(\vec{x}) \gamma_j (\psi^a(\vec{x}+\hat{k})[F_{jk}^{ab}(\vec{x}) + F_{jk}^{ab}(\vec{x}+\hat{k})]) - \{\psi^a(\vec{x}-\hat{k})[F_{jk}^{ab}(\vec{x}) + F_{jk}^{ab}(\vec{x}-\hat{k})]\}. \quad \text{(A1)}
\end{aligned}
$$

Similarly, for the 0^{--} P-wave source,

$$
\begin{aligned}
\mathcal{O}_P^{--} &= \sum_x \sum_{ijk} \epsilon_{ijk} \bar{\psi}^b \gamma_j (\vec{\partial}_k - \overleftarrow{\partial}_k) \psi^a F_{0i}^{ab} = \sum_x \sum_{ijk} \epsilon_{ijk} [\bar{\psi}^b(\vec{x}) \gamma_j \psi^a(\vec{x}+\hat{k}) F_{0i}^{ab}(\vec{x}) - \bar{\psi}^b(\vec{x}) \gamma_j \psi^a(\vec{x}-\hat{k}) F_{0i}^{ab}(\vec{x}) \\
&\quad - \bar{\psi}^b(\vec{x}+\hat{k}) \gamma_j \psi^a(\vec{x}) F_{0i}^{ab}(\vec{x}) + \bar{\psi}^b(\vec{x}-\hat{k}) \gamma_j \psi^a(\vec{x}) F_{0i}^{ab}(\vec{x})] \\
&= \sum_x \sum_{ijk} \epsilon_{ijk} [\bar{\psi}^b(\vec{x}) \gamma_j \psi^a(\vec{x}+\hat{k}) F_{0i}^{ab}(\vec{x}) - \bar{\psi}^b(\vec{x}) \gamma_j \psi^a(\vec{x}-\hat{k}) F_{0i}^{ab}(\vec{x}) \\
&\quad - \bar{\psi}^b(\vec{x}) \gamma_j \psi^a(\vec{x}-\hat{k}) F_{0i}^{ab}(\vec{x}-\hat{k}) + \bar{\psi}^b(\vec{x}) \gamma_j \psi^a(\vec{x}+\hat{k}) F_{0i}^{ab}(\vec{x}+\hat{k})] \\
&= \sum_x \sum_{ijk} \epsilon_{ijk} [\bar{\psi}^b(\vec{x}) \gamma_j (\psi^a(\vec{x}+\hat{k})[F_{0i}^{ab}(\vec{x}) + F_{0i}^{ab}(\vec{x}+\hat{k})]) - \{\psi^a(\vec{x}-\hat{k})[F_{0i}^{ab}(\vec{x}) + F_{0i}^{ab}(\vec{x}-\hat{k})]\}]. \quad \text{(A2)}
\end{aligned}
$$

[1] J. Sexton, A. Vaccarino, and D. Weingarten, Phys. Rev. Lett. **75**, 4563 (1995); in *Lattice '96*, Proceedings of the International Symposium, St. Louis, Missouri, edited by C. Bernard *et al.* [Nucl. Phys. B (Proc. Suppl.) **53**, 232 (1997)].

[2] G. Bali *et al.*, Phys. Lett. B **309**, 378 (1993).

[3] For a review see T. Barnes, F. E. Close, and E. S. Swanson, Phys. Rev. D **52**, 5242 (1995).

[4] L. A. Griffiths, C. Michael, and P. E. L. Rakow, Phys. Lett. **129B**, 351 (1983); S. Perantonis and C. Michael, Nucl. Phys. **B347**, 854 (1990).

[5] S. Catterall *et al.*, Phys. Lett. B **300**, 393 (1993).

[6] P. Lacock, C. Michael, P. Boyle, and P. Rowland, Phys. Rev. D **54**, 6997 (1996).

[7] C. Michael, in *Proceedings of the 10th Les Rencontres de Physique de la Vallee d'Aoste: Results and Perspectives in Particle Physics*, La Thuile, Italy, 1996, edited by Mario Greco

(Istituto Nazionale di Fisica Nucleare, Frascati, Italy, 1996), p. 932; P. Lacock, C. Michael, P. Boyle, and P. Rowland, Phys. Lett. B **401**, 308 (1997).

[8] C. Bernard *et al.*, in *Lattice '96* [1], p. 228.

[9] J. E. Mandula, Phys. Lett. **135B**, 155 (1984).

[10] See, for example, D. Horn and J. Mandula, Phys. Rev. D **17**, 898 (1978).

[11] C. Bernard *et al.*, in *Lattice '95*, Proceedings of the International Symposium, Melbourne, Australia, edited by T. D. Kieu *et al.* [Nucl. Phys. B (Proc. Suppl.) **47**, 345 (1996)].

[12] C. Bernard *et al.*, in *Lattice '96* [1], pp. 212 and 358.

[13] P. B. MacKenzie, in *Lattice '91*, Proceedings of the International Symposium, Tsukuba, Japan, edited by M. Fukugita *et al.*, [Nucl. Phys. B (Proc. Suppl.) **26**, 369 (1992)]; A. X. El-Khadra, *ibid.* p. 372; in *Lattice '92*, Proceedings of the International Symposium, Amsterdam, The Netherlands, edited

by J. Smit and P. van Baal [Nucl. Phys. B (Proc. Suppl.) **30**, 449 (1993)].

[14] C. Bernard *et al.*, Nucl. Phys. B (Proc. Suppl.) (to be published).

[15] P. R. Page, Phys. Lett. B (to be published); E. S. Swanson and A. P. Szczepaniak, hep-ph/9704434.

[16] Particle Data Group, R. M. Barnett *et al.*, Phys. Rev. D **54**, 1 (1996).

[17] X. Alde *et al.*, Phys. Lett. B **205**, 397 (1988).

[18] Y. D. Prokoshkin and S. A. Sadovskii, Phys. At. Nucl. **58**, 606 (1993).

[19] D. R. Thomson *et al.*, Phys. Rev. Lett. **79**, 1630 (1997).

[20] X. Alde *et al.*, Phys. Lett. B **216**, 447 (1989).

[21] X. Lee *et al.*, Phys. Lett. B **323**, 227 (1994).

[22] F. E. Close and P. R. Page, Phys. Lett. B **366**, 323 (1996).

[23] F. E. Close, Phys. Lett. B **342**, 369 (1995).